Plant-Based Antigen Production Strategy for SARS-CoV-2 Nucleoprotein and RBD, and Their Use for Detection of Antibody Responses in COVID-19 Patients

Katerina Takova , Valeria Tonova , Maria Pishmisheva , Stanislav Kotsev , Ivan Minkov , Eugenia S. Mardanova , Nikolai V. Ravin , Gergana Zahmanova *

Posted Date: 18 November 2024

doi: 10.20944/preprints202411.1268.v1

Keywords: SARS-CoV-2; receptor-binding domain (RBD); nucleoprotein (N); hepatitis E virus capsid protein; detection of serum antibodies; transient expression; plant molecular farming; diagnostic antigen

Article

Plant-Based Antigen Production Strategy for SARS-CoV-2 Nucleoprotein and RBD, and Their Use for Detection of Antibody Responses in COVID-19 Patients

Katerina Takova [1,†], Valeria Tonova [1,2,†], Ivan Minkov [2,3], Eugenia S. Mardanova [4], Nikolai V. Ravin [4], Stanislav Kotsev [5], Maria Pishmisheva [5] and Gergana Zahmanova [1,2,*]

[1] Department of Molecular Biology, University of Plovdiv, Plovdiv, 4000, Bulgaria
[2] Department of Technology Transfer and IP Management, Center of Plant Systems Biology and Biotechnology, Plovdiv, 4000, Bulgaria
[3] Institute of Molecular Biology, Markovo, 4023, Bulgaria
[4] Institute of Bioengineering, Research Center of Biotechnology of the Russian Academy of Sciences, 119071 Moscow, Russia
[5] Department of Infectious Diseases, Pazardzhik Multiprofile Hospital for Active Treatment, Pazardzhik, 4400, Bulgaria
* Correspondence: gerganaz@uni-plovdiv.bg
† These authors contributed equally to this work.

Featured Application: Plant-produced SARS-CoV-2 nucleoprotein (N) and chimeric receptor-binding domain (RBD) presented by hepatitis E virus capsid protein (HEV/RBD) are reliable as diagnostic antigens in serological tests for detection of antibody responses in COVID-19 patients. We propose a plant-based HEV/RBD iELISA assay which was able to detect anti-RBD IgG in human serum with a very high agreement of 91.66% and Cohen's k: 0.8316 compared to the commercially available ELISA COVID-19 IgG kit. Further, we developed Double Recognition iELISA based on HEV/RBD and N protein with a sensitivity 85.42%, and specificity of 94.44%.

Abstract: During the current severe acute respiratory syndrome coronavirus 2 (SARS-CoV-2) pandemic, the rapid development of efficient and sensitive serological tests for monitoring the dynamics of the disease as well as the immune response after illness or vaccination was critical. In this regard, low-cost and fast production of immunogenic antigens is essential for the rapid development of diagnostic serological kits. This study assessed the plant-based production of nucleoprotein (N) of SARS-CoV-2 and chimeric receptor-binding domain (RBD) of SARS-CoV-2 presented by hepatitis E virus capsid (HEV/RBD) and validation of the plant-derived proteins as diagnostic antigens for serological tests. The hepatitis E virus capsid protein was used as a carrier of RBD because of its ability to be expressed in plants in huge amounts and spontaneously assemble into higher order structures stabilizing inserted foreign immunogenic peptides. The N and chimeric HEV/RBD were expressed in and extracted from *Nicotiana benthamiana* plants and purified through immobilized metal-anion chromatography (IMAC). The resulting protein yield of chimeric HEV/RBD protein reached 100 mg/kg fresh weight, and 30 mg/kg fresh weight for N protein. Mass photometry analysis revealed that the N protein mainly forms tetramers, for HEV/RBD, results suggest that the fusion protein is largely monomeric. The purified N protein and HEV-RBD protein were used to develop an indirect enzyme-linked immunosorbent assay (iELISA) for the detection of antibodies to SARS-CoV-2 in human sera. To validate the iELISA tests, a panel of 84 sera from patients diagnosed with COVID-19 was used, and the results were compared to those obtained by another commercially available ELISA Kit (Dia.Pro D. B., Italy). The performance of an HEV/RBD in-hose ELISA showed a sensitivity of 89.58% (95% Cl: 75.23-95.37) and a specificity of 94.44% (95% Cl: 76.94-98.2). Double Recognition iELISA based on HEV/RBD and N protein is characterized by a lower sensitivity of 85.42% (95% Cl: 72.24-93.93), and specificity of 94.44% (95% Cl: 81.34-99.32) at cut-off = 0.154, compared with iELISA based on HEV/RBD. Our study confirms that the transiently expressed in plants N and fusion HEV/RBD proteins can be used to detect responses to SARS-CoV-2 in human sera reliably. Our research validates the commercial potential of using plants as an expression system for recombinant protein production and their application as diagnostic reagents for serological detection of infectious diseases, hence lowering the cost of diagnostic kits.

 doi:10.20944/preprints202411.1268.v1

Keywords: SARS-CoV-2; receptor-binding domain (RBD); nucleoprotein (N); hepatitis E virus capsid protein; detection of serum antibodies; transient expression; plant molecular farming; diagnostic antigen;

1. Introduction

The highly dynamic epidemiological environment with changing viral pathogens requires constant research on emerging pathogens, their diagnosis, and prevention. The COVID-19 pandemic highlighted the demand for a rapid response from pharma companies to effectively produce large amounts of compounds to protect, treat, and diagnose new viral diseases. This global crisis has accelerated scientific advancements, facilitated cross-disciplinary cooperation, and enabled an agile advancement of technology. Recombinant proteins for application in pharmacy and medicine can be produced using a variety of expression systems, including bacteria, yeast, plants, insects, or animal cells [1–5]. Plants have been proven cost-effective, easily scaled up, safe, and valuable in the production of high amounts of proteins, under conditions of urgency, such as emerging viruses [6–10]. The constant progress of biotechnology, plant cell cultures, agroinfiltration-based transient expression systems, and recombinant protein downstream processing help the plant molecular farming industry improve the current expression platforms and provide more effective solutions for recombinant protein production [11–14]. Plant expression systems become a competitive "biofactory" for producing valuable pharmaceuticals [15–17].

During the SARS-CoV-2 pandemic, the rapid development of efficient and sensitive serological tests for monitoring the dynamics of the disease as well as the immune response after illness or vaccination was critical. Since the spike (S) and nucleoprotein (N) of SARS-CoV-2 are the most immunogenic proteins, serological testing usually identifies antibodies against these two proteins [18,19]. The S protein is composed of two subunits, S1 and S2, and is used by the virus to attach itself to ACE-2 (angiotensin-converting enzyme 2) host cell receptor[20]. The S1 contains the surface-exposed receptor binding domain (RBD) that specifically recognizes the host cell receptor to gain entry into the cell and fuse viral and lysosomal membrane [21]. The N protein is responsible for wrapping the virus RNA and forming ribonucleoprotein complex (RNP), and it has been highly expressed during infection, inducing early humoral and cellular response [22]. N is 45.6 kDa phosphoprotein composed of two domains, N terminal domain (NTD) and C terminal domain (CTD) linked with intrinsically disordered amino acid stretches [23]. N protein is highly conserved, possessing 89.7% homologous to the N of SARS-CoV-1 [24–26]. N protein is abundantly expressed during the infection, inducing early humoral and cellular immune responses [27]. Antibodies against the N protein are intensely generated during infection, even though they lack neutralizing activity they may be used for serological diagnosis [28,29].

It has been proposed that antibodies targeting the S protein are more specific and an accurate indicator of protective immune response, while those against N are more sensitive, at the expense of specificity (N protein of SARS-CoV-2 has high protein sequence similarity with the other *Coronaviridae* nucleocapsid proteins [30].

As a fusion protein or alone, RBD was produced in plants with its maximal purifying yield of approximately 40 μg per gram of fresh leaf tissue [31–33]. To increase the yields and stability of RBD, the RBD was fused to the truncated capsid protein of the hepatitis E virus at the Tyr485 position [34]. The capsid protein of HEV can self-assemble into virus-like particles (VLPs) when expressed in *Nicotiana benthamiana* plants and can be used as a carrier of immunogenic proteins[35,36]. Further, we applied the strategy to target the fused HEV/RBD protein to the endoplasmic reticulum (ER), which can influence the expression efficiency of the recombinant proteins, its stability, and solubility [37].

Numerous quantitative serological tests have been created to assess the antibody titers in sera, primarily based on N and S proteins of SARS-CoV-2 [38,39]. In this regard, low-cost and fast production of these immunogenic antigens is essential for the rapid development of diagnostic

 doi:10.20944/preprints202411.1268.v1

serological kits, and plant-based expression systems can offer that. We transiently expressed the main immunogenic proteins from SARS-CoV-2, the nucleoprotein, and the receptor-binding domain (RBD) bearing from hepatitis E virus capsid protein in *Nicotiana benthamiana* plants. We proved the efficient production and purification of N and chimeric HEV/RBD proteins and demonstrated their suitability to recognize anti-SARS-CoV-2 antibodies in COVID-19 patients using iELISA test.

2. Materials and Methods

2.1. Gene preparation, cloning of Nucleocapsid (N) in pEAQ-HT, and Agroinfiltration of Nicotiana benthamiana

The nucleotide sequences of the whole Nucleocapsid (N) of SARS-CoV-2 strain Wuhan-Hu-1 (GenBank accession number: MN908947.3) with six-histidine tag in its C-terminus were plant condones optimized and synthesized by GenScript Biotech (Piscataway, New Jersey, USA). The N-C 6his tag gene was cloned into pEAQ-*HT* [40] using the restriction sites *Age*I/*Xho*I . The construct pEff-HEV/RBD containing the RBD (from V319 to V524) of SARS-CoV-2 strain Wuhan-Hu-1 (GenBank QJE37812.1) and HEV capsid protein 110-610 (GenBank accession number DQ079627.1) was produced as previously described by our groups [34,35]. Briefly, the recombinant plasmids pEAQ-*HT*-N and pEff-HEV/RBD were transformed into competent *Escherichia coli* XL1Blue; putative clones harboring the expression vectors (pEAQ-*HT*-N and pEff-HEV/RBD) were verified by sequencing (Eurofins, Hamburg, Germany). Recombinant vectors were transformed into the electrocompetent *Agrobacterium tumefaciens* strain LBA4404.

2.2. Transient expression of N and HEV/RBD in Nicotiana benthamina

The recombinant agrobacterial clones were cultured in a Luria–Bertani medium containing 50 μg/mL Kanamycin and 100 μg/mL Rifampicin, for 16 hours at 28 °C. The culture was then pelleted. The obtained bacteria were resuspended in an infiltration solution containing 10 mM MES 2-(N-morpholino) ethansulfonic acid with a pH of 5.5, 10 mM $MgSO_4$, and 100 μM acetosyringone. Bacterial suspensions (OD_{600} of 0.2) were syringe- or vacuum-infiltrated into the leaves of four–five-week-old *N. benthamiana* plants. Leaves were harvested 4 days after infiltration (dpi)[34].

2.3. Purification of Plant-Produced N and HEV/RBD Using Affinity chromatography

Large-scale sampling was conducted by removing non-infiltrated tissue and recording leaf sample weight. Samples were extracted by adding 3 volumes of the PBS pH 7.2 extraction buffer with complete EDTA-free protease inhibitor cocktail tablets (Roche Diagnostics GmbH, Mannheim, Germany), and were then mechanically homogenized. The N protein carrying the C-terminal 6-histidine tag and the HEV/RBD protein carrying the C-terminal 8-histidine tag and ER-retention signal were isolated under native conditions, using immobilized metal-anion chromatography (IMAC) on a Ni-NTA column, according to the manufacturer's instructions (Qiagen, Hilden, Germany). The eluted protein was dialyzed against PBS pH 7.2, and four buffers were changed using Slide-A-Lyzer Mini dialysis devices (Thermo Fisher Scientific, Waltham, MA, USA). The proteins were quantitated using a Qubit Fluorometer (Thermo Fisher Scientific, Waltham, MA, USA) with a Qubit Protein Assay Kit, following the manufacturer's instructions.

2.4. SDS-PAGE and Western Blot of Plant-Produced N and HEV/RBD

SDS-PAGE was carried out using NuPAGE Bis-Tris Mini gels of 4–12% (*w*/*v*) or 12% (*w*/*v*) acrylamide (Invitrogen, Carlsbad, CA, USA); protein prestained standard SeeBluePlus 2 (Invitrogen, Carlsbad, CA, USA) was used as a size marker throughout the experiments. To load a protein extract from 3 mg FW, 10 μL of sample solution was applied to an SDS-PAGE gel. Protein bands in the gels were visualized by Instant Blue (Expedeon, Cambridge, UK) staining. For the Western blot assay, the proteins were transferred from the SDS-PAGE gel onto a nitrocellulose membrane (Bio-Rad Laboratories Ltd, Hertfordshire, UK). Membranes were blocked with 5% (*w*/*v*) nonfat dried milk in

 doi:10.20944/preprints202411.1268.v1

PBS with 0.05% Tween-20 (*v*/*v*) (PBST) and incubated for 1 h with mouse monoclonal antibodies against RBD (Xema, Moscow, Russia) at a dilution of 1:10,000 (2 mg/mL). The bound antibody was detected with secondary rabbit anti-mouse antibodies conjugated with horseradish peroxidase (HRP) (Promega, Madison, WI, USA at a dilution of 1:10,000. The emitted luminescence from the ECL detection reagents (GE Healthcare Life Sciences, Buckinghamshire, UK) was detected with the ImageQuant LAS 500 system (GE Healthcare Life Sciences, Buckinghamshire, UK).

2.5. Mass Spectrometry

Maldi-TOF/MS was used for the identification of N and HEV/RBD proteins. MS/MS analysis was performed as follows: The protein bands corresponding to the N protein and HEV/RBD were excised from the SDS-PAGE gel and washed with water, and then twice with water/ACN (1:1 *v*/*v*). The solvent volumes were about twice the volume of the gel. The liquid was removed and the gel pieces were rehydrated in 0.1 M NH4HCO3 for 5 min. ACN was added to give a 1:1 *v*/*v* mixture of 0.1 M NH4HCO3/CAN and left to stand for 15 min. All liquid was removed and the digestion buffer containing 25 mM NH4HCO3 and 10 ng/µL of trypsin was added. The mixture was then incubated for 4 h at 37 °C. The supernatant was recovered and the extraction was carried out with 1% TFA/ACN (1:1 *v*/*v*). Tryptic peptides were targeted for MALDI-TOF-MS, MS/MS, and a database search was performed.

2.6. Mass Photometry of N and HEV/RBD

Mass photometry measurements were performed at 25°C using a Refeyn OneMP mass photometer (Refeyn Ltd, UK). Calibration of the instrument was carried out with a NativeMark Unstained Protein Standard (Thermo Scientific), containing proteins ranging from 20 to 1,200 kDa. Standard calibration points were generated using proteins with masses of 146, 480, and 1,048 kDa.

The protein sample was purified in PBS buffer as described previously and concentrated to 200 nM. A 2 µL aliquot of the protein solution was mixed with 8 µL of buffer on a glass coverslip, resulting in a final concentration of approximately 50 nM. Data acquisition was carried out using AcquireMP software (version R1) over 60 seconds, with a frame rate of 60 frames per second and a large field of view.

Data analysis was performed using DiscoverMP software (version R1.2). Protein mass was estimated by fitting a Gaussian distribution to the mass histograms, and the mode of the distribution was used as the representative mass.

2.7. Serum Samples

A panel of 84 serum samples from patients with proven COVID-19 with nasal COVID-19 Ag test (SD Biosensor, Suwon, Republic of Corea) were collected between 5-7 days after first symptoms in Pazardzhik Multiprofile Hospital for Active Treatment. All patients have a signed informed consent. 11 pre-pandemic serum samples (collected before November 2019) were stored at -20 °C and used as negative controls. The study was approved by the IMBB institutional ethics committee (process number EK04-06062023).

2.8. Commercial anti-Spike 1(RBD)/2 IgG ELISA Kit (Dia.Pro D. B., Italy)

ELISA Kit (Dia.Pro D. B., Italy) was used to analyze the serum samples from 84 patients with proven COVID-19, following the manufacturer's instructions.

2.9. Optimization of indirect iELISA Protocol Based on HEV/RBD or N Recombinant Protein

A total of 5 negative and 5 positive serum samples, randomly selected from previously evaluated samples, were tested in two independent experiments. Optimal working dilutions of the coating N or HEV/RBD recombinant proteins have been determined. Briefly, well plates were coated with 2, 5, and 10 µg/mL of the recombinant protein in Bicarbonate/carbonate coating buffer (100 mM) with a pH of 9.6. The microtiter plates (Maxisorp 96-well flat bottom) were coated with 100 µL/well of

 doi:10.20944/preprints202411.1268.v1

purified coating protein and incubated overnight at 4 °C. After three washes with PBST, the plates were incubated with 200 µL/well of blocking solution (PBST–3% [*w*/*v*] BSA) for 1 h at room temperature. Aliquots of sera diluted at 1:40 in blocking buffer were dispensed into the wells of the plates and incubated for one hour at 37 °C. After three washes with PBST, the HRP-conjugated goat anti-human secondary antibody (ThermoFisher Scientific, Waltham, MA, USA) was added at a dilution of 1:10,000. After incubation with the secondary antibody, plate wells were washed three times before 50 µL/well of the substrate solution (*o*-phenylenediamine, Millipore–Sigma, Munich, Germany) was added. Plates were incubated in the dark at room temperature for 20 min. The reaction was stopped with 50 µL 1 M H_2SO_4, and the plates were read at 492 nm in an Epoch Microplate Spectrophotometer plate reader (BioTek Instruments Inc., Winooski, VT, USA). Mean positive/negative (P/N) ratio was calculated.

2.10. Statistical Analysis, and Cut-off Evaluation of the iELISA

Excel Microsoft program was used to find the most appropriate cut-off value, receiver operated characteristic (ROC), specificity, sensitivity, efficiency, and area under the curves (AUCs). The agreement between the Commercial anti-Spike 1(RBD)/2 IgG ELISA Kit (Dia.Pro D. B., Italy), and the in-house assays was assessed by pairwise comparisons between the degree of accuracy and reliability in statistical classification (kappa coefficient).

3. Results

3.1. Gene cloning, Production, and Purification of N and HEV/RBD recombinant proteins

The plant codone optimized N gene was cloned into a pEAQ-*HT* vector using *Age* I and *Xho* I restriction sites (Figure 1, a). The plant codone-optimized HEV/RBD gene was cloned into pEff vector (Figure 1, b) [34]. HEV/RBD expression was targeted to the endoplasmic reticulum (ER). We obtained this purpose by adding ER-targeting signal peptide at the N-terminus and ER retention signal HDEL at the C-terminus of the fusion protein [34]. To facilitate the purification of the N and HEV/RBD recombinant proteins, a 6-histidine tag and an 8-histidine tag were added to the C-terminus of the N and HEV/RBD recombinant proteins, respectively (Figure 1). The sequences of the inserts were confirmed by sequencing and the recombinant vectors were transformed into *A. tumefaciens* and used to infiltrate *N. benthamiana* leaves.

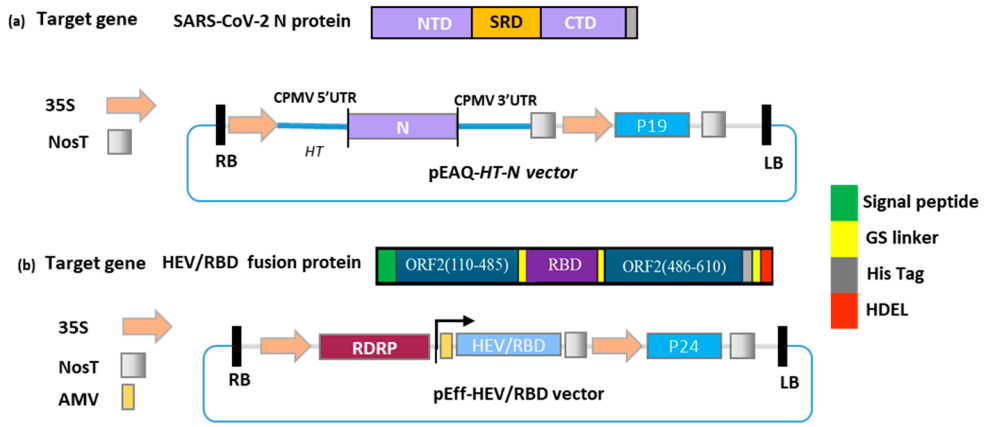

Figure 1. Scheme of the recombinant vectors pEAQ-*HT*-N (a) and pEff-HEV/RBD (b). 35S, promoter of the cauliflower mosaic virus RNA; NosT, terminator of the nopaline synthase gene from *A. tumefaciens*; P24, P19, gene of silencing suppressor from grapevine leafroll-associated virus-2 and from the Tomato bushy stunt (Tombus) group virus, respectively; LB and RB are the left and right borders of T-DNA; 5′-UTR from cowpea mosaic virus RNA-2; 3′-UTR from cowpea mosaic virus RNA-2; RDRP, RNA-dependent RNA polymerase of PVX; Sgp1, the first promoter of the subgenomic RNA of PXV; AMV, the leader sequence of RNA 4 of alfalfa mosaic virus.

 doi:10.20944/preprints202411.1268.v1

N. benthamiana leaves were agroinfiltrated with the recombinant vectors pEAQ-*HT*-N and pEff-HEV/RBD. The morphological changes were observed in the plant leaves agroinfiltrated with *Agrobacterium* carrying pEff-HEV/RBD. The leaves started to show serious necrosis at 5 dpi (Figure 2a). In plants agroinfiltrated with pEAQ-HT-N chlorosis began on the base leaves at 5 dpi (Figure 2b).

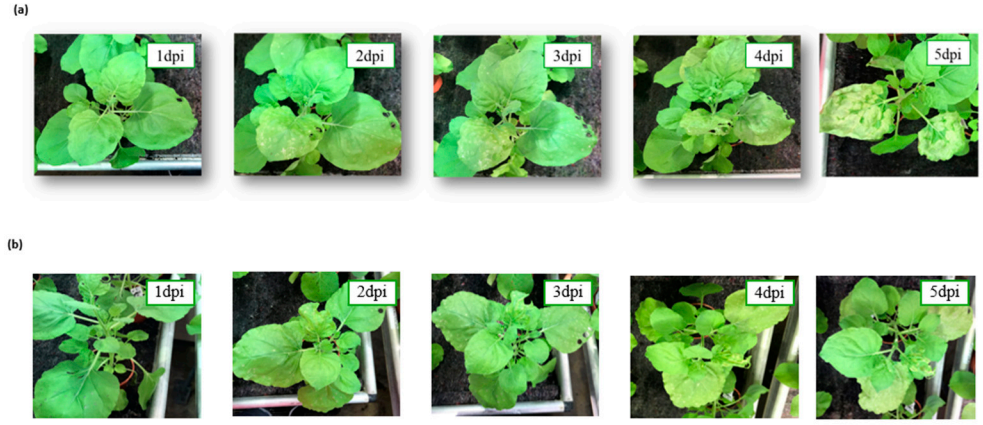

Figure 2. Morphological changes of *N. benthamiana* leaves after agroinfiltration with Agrobacterium carrying pEff-HEV/RBD construct (a); *N. benthamiana* leaves after agroinfiltration with Agrobacterium carrying pEAQ-HT-N construct.

Leaf tissues for isolation of protein samples were harvested four days after agroinfiltration based on the morphological characteristic of infiltrated leaves and expression analyses (data not shown). The HEV/RBD and N proteins purification were performed using metal-affinity chromatography under native conditions. After purification, the protein samples were dialyzed against PBS and were subject to SDS-PAGE gel analysis stained with Coomassiee Blue. The SDS-PAGE revealed that HEV/RBD fusion protein is expressed very well in plants (Figure 3a), and we observed a massive band of 81 kDa fusion protein. The Western blot analysis with an anti-RBD mAb further confirms the presence of HEV/RBD protein. (Figure 3b). The IMAC method applied here obtained the ~100 mg HEV/RBD of kg fresh tissue weight (FW).

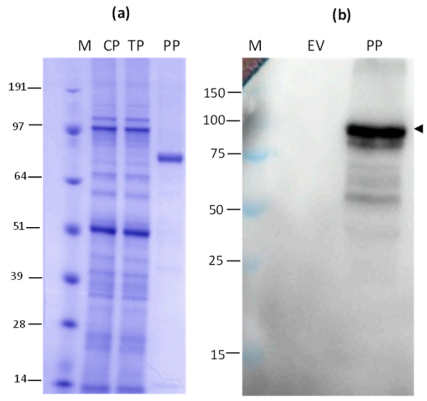

Figure 3. (a) SDS-PAGE Coomassie brilliant blue-stained gel of HEV/RBD fusion protein. (b) Western blot with a monoclonal anti-RBD mAb. M-prestained protein molecular marker (kDa), The position of HEV/RBD protein (calculated molecular weight 81 kD) is shown by a black arrow. M-protein molecular marker; CP, a total soluble protein isolated from the infiltrated leaf with pEff-HEV/RBD before filtration; EV, a total soluble protein extracted from plant leaves infiltrated with empty pEff. TP, a total soluble protein extracted from plant leaves inoculated with pEff-HEV/RBD after filtration with 45 µm filter; PP, IMAC purified protein.

 doi:10.20944/preprints202411.1268.v1

The *N. benthamiana* leaves infiltrated with pEAQ were harvested on 4 dpi and recombinant N protein was purified by IMAC. The purified N protein was analyzed by SDS PAGE (Figure 4a) and Western blot with anti-his Ab (Figure 3b). The purified N protein was observed as a monomer (49.5 kDa), dimer, and tetramer (Figure 4a). The final yield of the N protein after purification was about 30 mg/kg of WF.

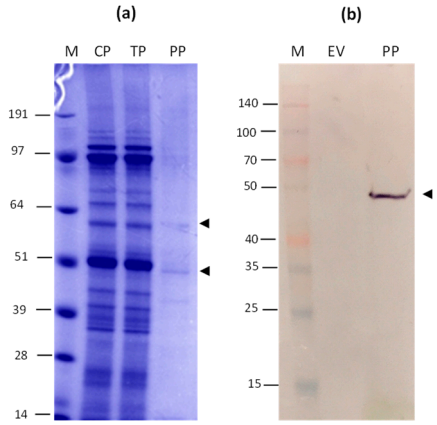

Figure 4. Expression of and N proteins in *N. benthamiana* plants (4 dpi). (a) The IMAC purified N protein was analyzed by SDS PAGE followed by Coomassie brilliant blue-stained; (b) The N protein was analysed by Western blot probed with anti-His tag Ab. M, molecular weight marker (sizes in kD); CP, total protein isolated from the infiltrated leaf before filtration; TP, total proteins isolated from infiltrated leaf after filtration with 45 µm filter; PP, IMAC purified N protein; EV, total proteins isolated from the infiltrated leaf with empty vector.

3.2. Mass Spectrometry

Mass Spectrometry analysis confirmed the identity of the purified N and HEV/RBD proteins by comparing the masses of peaks obtained with MALDI-TOF MS (Figure S1 supplementary file).

3.3. Mass photometry (MP)

We used mass photometry (MP) to directly measure the molecular weight distribution of N and HEV/RBD proteins in solution. For the N protein, a majority peak can be discerned approximately at the tetramer mass (Figure 5a) and bigger oligomers (Figure 5b). N creates tetramers through disulfide cross-links of noncovalent dimers, as was previously demonstrated[41].

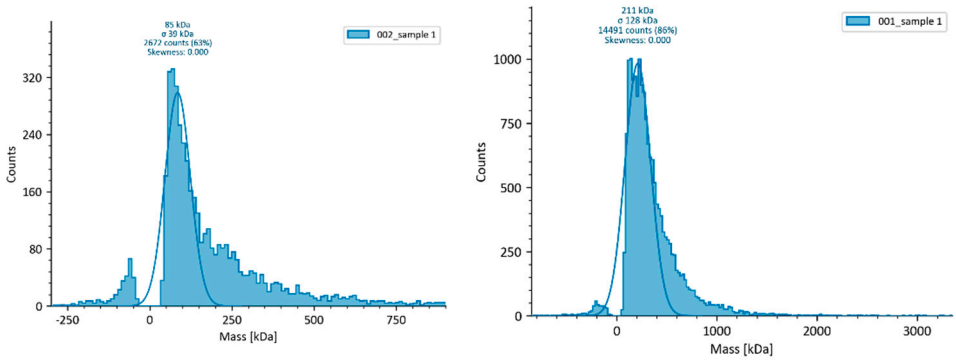

Figure 5. Determination of mass distribution by MP of N protein expressed and purified from plants. MP was shown as histograms of the masses associated with single molecule surface adsorption events of the N protein in PBS buffer.

MP shows that the HEV/RBD fusion protein expressed and purified from plants is largely monomeric in PBS buffer (Figure 6).

 doi:10.20944/preprints202411.1268.v1

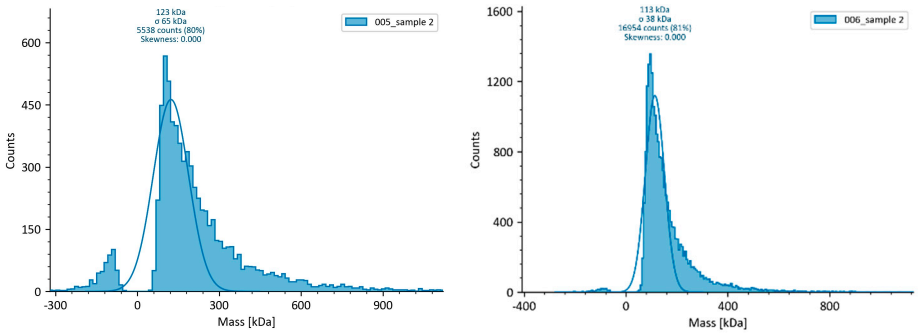

Figure 6. Determination of mass distribution by MP of HEV/RBD protein expressed and purified from plants.

3.3. iELISA optimization using the plant-derived HEV/RBD and N

The plant-derived recombinant proteins were used to develop an iELISA to test anti-N or anti-RBD antibodies in human sera. The optimal concentration of the recombinant proteins to coat the iELISA plate was 5 µg/mL for HEV/RBD protein and 10 µg/mL for N protein; serum dilution - 1:40, II Ab (anti-IgG) - 1:10 000. The optimal conditions were determined based on the optimal relation between the positive and the negative samples (P/N) in the different coating antigen concentrations (Figure S2 supplementary file).

The sensitivity, specificity, and cut-off value of the iELISA were determined by testing 84 serum samples from hospitalized patients with proven SARS-CoV-2 diagnosis with fast COVID-19 Ag test and 11 serum samples collected before the COVID-19 pandemic. The assay cut-off value (A492 nm = 0.139) was determined as a 3x standard deviation (SD) above the mean optical density of pre-pandemic sera (Figure 7).

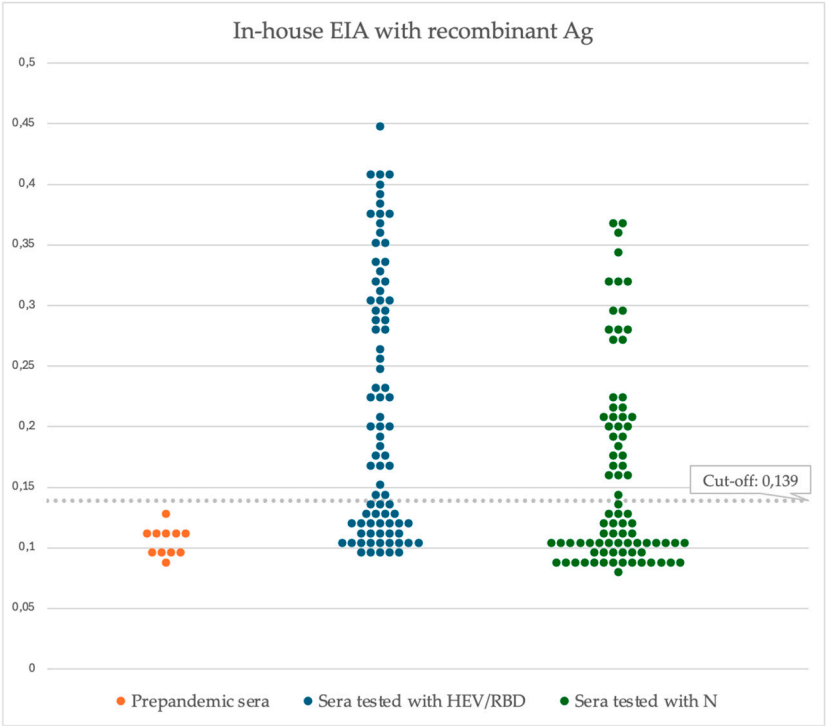

Figure 7. Plant-derived SARS-CoV-2 N and HEV/RBD protein detect IgG in serum samples from COVID-19 hospitalized patients (n=84), indicated in blue and green. Results are presented as the optical density value (OD) of analysed serums. A cut-off for positivity was determined as 3xSD (standard deviation) above the mean optical density of pre-pandemic sera (n=11) indicated in orange.

 doi:10.20944/preprints202411.1268.v1

Furthermore, the HEV/RBD coating Ag was analysed by serum samples (n=6) negative for anti-S IgG and positive for anti-HEV IgG. The results from iELISA test show that anti-HEV-specific antibodies recognized the HEV/RBD Ag (Figure S3 supplementary). The retained antigenicity of HEV capsid protein fused with RBD can be an obstacle to the correct evaluation of the anti-RBD iELISA specificity.

3.4. Receiver Operating Characteristic (ROC), specificity, and sensitivity of in-house ELISA with plant-derived HEV/RBD protein

The Receiver Operating Characteristic (ROC) curve was generated using the results obtained by analyzing 36 negative and 48 positive human serum samples (n=84), previously tested by a commercial anti-Spike 1(RBD)/2 IgG ELISA Kit (Dia.Pro D. B., Italy). Notably, a comparison between iELISA (HEV-RBP) and a validated, high-sensitivity commercial ELISA kit showed a sensitivity of 89.58% (95% Cl: 77.34-96.53) and a specificity of 94,44% (95% Cl: 81.34-99.32). The assay cut-off value (A492 nm = 0.175) was determined as the optimal value of sensitivity and specificity (Figure 8). The area under the curve (AUC) is 0.943.

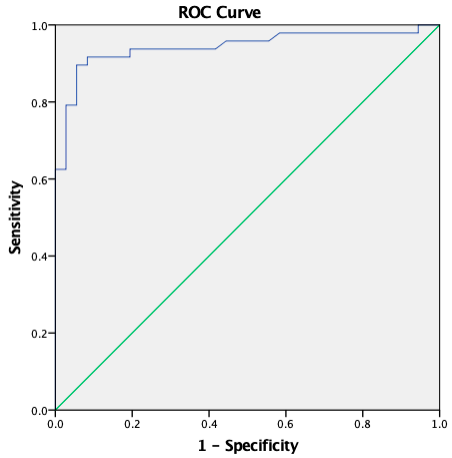

Figure 8. ROC analysis of iELISA based on HEV/RBD coating Ag (5 µg/mL). The area under the curve (AUC) is 0.943.

The comparison between the two variants of cut-off and a summary of the performance of the HEV/RBD-based iELISA is presented in Table 1.

Table 1. The performance of HEV/RBD based IgG ELISA and comparison between the two variants of cut-off analysis.

	Mean negative OD + 3SD	ROC curve
Cut off	0.139	0.175
True Positive	45/48	43/48
True Negative	29/36	34/36
Sensitivity	93.75% [82.8-98.69]	89.58% [77.34-96.53]
Specificity	80.56% [63.98-91.81]	94.44% [81.34-99.32]
Accuracy	88.10% [79.19-94.14]	91.67% [83.58-96.58]
Positive Predictive Value	86.54% [76.71-92.62]	95.56% [84.78-98.81]
Negative Predictive Value	90.62% [76.16-96.69]	87.18% [74.72-93.99]

The comparison between the anti-Spike 1(RBD)/2 IgG ELISA Kit (Dia.Pro D. B., Italy) commercial kit and the in-hose ELISA is presented in Table 2.

 doi:10.20944/preprints202411.1268.v1

Table 2. Performance of agreement between the anti-Spike 1(RBD)/2 IgG ELISA Kit (Dia.Pro D. B., Italy) commercial kit and the in-hose ELISA in the detection of anti-RBD IgG. 84 serum samples were tested in duplicates with the commercial and iELISA tests.

		Commercial EIA		
		Positive	Negative	Total
iELISA	Positive	43	2	45
	Negative	5	34	39
	Total	48	36	84
Kappa index	0.8316			

Comparison between the commercial anti-Spike 1(RBD)/2 IgG ELISA Kit (Dia.Pro D. B., Italy) commercial kit and iELISA are characterized with a high agreement of 91.66% and Cohen's k: 0.8316 between the results of the two methods. Of the 84 tested serums, the commercial kit identified 49 positive and 36 negative samples. Of the 48 positive samples, 43 were also identified as positive by the iELISA (sensitivity of 89.58%). The remaining 5 we identified as negative samples. 34 of the 36 negative samples were identified as negative by iELISA (specificity of 94.44%). Overall, 7 of the 84 analyzed samples showed conflicting results (Table 2).

3.4. ROC, specificity and sensitivity of the in-house Double Recognition iELISA based on HEV/RBD and N

Double Recognition iELISA used HEV/RBD and N protein as coating antigens for double recognition of anti-RBD Ab and anti-N Ab in human serum. All human serums (n=84) were tested by double Recognition iELISA, which was characterized by a sensitivity of 85.42% (95% Cl: 72.24-93.93), and specificity of 94.44% (95% Cl: 81.34-99.32) at cut-off = 0.154 (Figure 9).

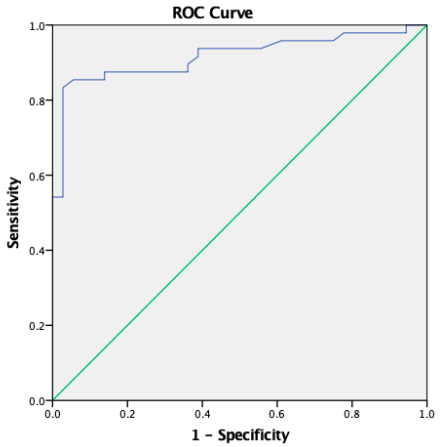

Figure 9. ROC analysis of double recognition Immunoassay (HEV/RBD 5 μg/mL + N 5 μg/mL). The area under the curve (AUC) is 0.917.

4. Discussion

The availability of efficient expression systems for the rapid and efficient production of immunogenic proteins is critical in the fight against emerging infectious diseases. Using sensitive and affordable diagnostic kits makes it possible to carry out large-scale seroepidemiological studies in humans and susceptible animal species to emerging infections. In this study, we report the usefulness of the plant expression system in large-scale and cost-effective production of SARS-CoV-2 nucleoprotein and fusion HEV/RBD protein and their application in serological tests for detecting antibody responses in COVID-19 patients. We describe the development of an indirect in-house ELISA using the fusion HEV/RBD protein as a coating antigen. Further, we reported the establishment of a double recognition immunoassay based on two antigens (N and HEV/RBD) of SARS-CoV-2. Finally, we compared the specificity and sensitivity of the iELISA tests with the validated commercial ELISA COVID-19 S1-S2 IgG kit (Dia.Pro D. B., Italy).

 doi:10.20944/preprints202411.1268.v1

Nucleoprotein was selected because it is shown to be the most abundantly expressed protein during SARS-CoV-2 infection and a highly immunogenic [42,43]. The antibodies produced against N are unlikely to neutralize SARS-CoV-2 directly [44]. RBD, on the other hand, is the primary target for neutralizing antibodies, and the demonstration of such antibodies indicates the presence of a protective immune response [45]. Since each of these proteins has advantages and disadvantages as diagnostic antigens, using them all together will most likely give an overall picture. Additionally, people who receive S-based vaccinations do not have antibodies to N protein [46].

There are many different heterologous expression systems including *E. coli*, yeast, insect cells, mammalian cells, and plants for the expression of highly specific detection probes in research and diagnostics, each with specific benefits and drawbacks [47–51]. Theoretically, plant expression systems have several advantages: plants can be used for the production of large amounts of high-quality recombinant proteins, with similar posttranslational modifications (PTMs) as mammalian cells, utilized to detect, and treat several viral disease s. Leafy crops like *Nicotiana benthamiana* can be cultivated under controlled conditions and grown to agricultural size generating significant amounts of biomass. *N. benthamiana* has been used for transient expression, providing a higher yield of recombinant proteins within a shorter timeline and successfully applied as a rapid response platform addressing emerging viral diseases [35,52,53]. There are several challenges in producing diagnostic Ag in plants. Various techniques have been used to overcome the glycosylation pattern-induced product heterogeneity and proteolytic degradation of recombinant proteins [54,55]. PTMs play a significant role in the efficacy of plant-derived diagnostic reagents and affect antigen recognition and sensitivity of diagnostic tests. The SARS-CoV-2 structural proteins are extensively glycosylated[56], mostly the glycans are made up of complex-type N- and high-mannose type-glycans [33,57]. Nonetheless, high-mannose glycans' structure is universal throughout eukaryotes, which may lessen the variations between RBD generated by plants and mammals [58].

Here we used transiently transformed *N. benthamiana* to produce an HEV/RBD fusion protein and N protein to set up an iELISA test for serological analysis of serum samples from COVID-19 patients. The time requested for the expression and purification of the N and HEV/RBD diagnostic reagents was estimated to be 5-6 weeks, starting with *N. benthamiana* seeds germination and plant growth till recombinant protein extraction and purification. Plant leaves infiltrated with pEff-HEV/RBD resulted in the expression of an 81 kDa fusion HEV/RBD protein at up to 100 mg/kg of FW. Agroinfiltration of *N. benthamiana* with pEAQ-HT-N resulted in the expression of a 49.5 kDa N protein at up to 30 mg/kg of FW. The N protein is expressed in a lower but still satisfactory amount. In this study, the optimal conditions for iELISA were set at 5 μg/mL for HEV/RBD coating antigen and 10 μg/mL for N coating antigen, with a final volume used in the assay of 100 μL (equal to 0.5 μg/well and 1 μg/well respectively). The amount of ~50 μg is needed for coating a whole 96-well plate for HEV/RBD and ~100 μg for N protein. In *E. coli* expression, it has been reported that 1.5 mg of RBD protein can be produced per liter culture [59]. Using the same protocol, 1 L of culture would produce enough protein to process 3,000 samples, while 1 kg of FW plant leaves could produce enough protein to process 200,000 samples at the HEV/RBD fusion yield described herein. The IMAC purification steps allow the obtaining of recombinant proteins (N and HEV/RBD) with very high purity (Figure 3a, Figure 4a). The HEV/RBD and N recombinant proteins were proven to be recognized by commercially available ant-RBD mAb and anti-his tag mAb (Figure 3a, Figure 4a), respectively. Furthermore, the recombinant proteins were identified by MALDI-TOF and analyzed by mass photometry. As previously shown, we demonstrated that the plat-derived N protein forms tetramers. The tetramers are the results of disulfide cross-links of noncovalent N dimers [41]. Dimerization of SARS-CoV-2 nucleoprotein affects the sensitivity of ELISA based on N protein for serological diagnostics of COVID-19 [60]. Previously, we demonstrated that the HEV/RBD can assembled into high-order structures [34]. Here, the mass photometry analysis shows that the HEV/RBD fusion protein is largely monomeric in PBS buffer, and does not form virus-like particles (VLPs). We demonstrated that the assembly and stability of HEV capsid VLPs are lower and depend on the purification method, buffer conditions, and the position of the inserted foreign protein [51,61]. A panel of 84 sera from patients diagnosed with COVID-19 was used to assess the recognition between

 doi:10.20944/preprints202411.1268.v1

plant-derived antigens and serum antibodies. The results from HEV/RBD-based iELISA and double recognition ELISA (based on N and HEV/RBD) were compared to those obtained by commercially available ELISA COVID-19 S1-S2 IgG kit (Dia.Pro D. B., Italy). The agreement between the HEV/RBD-based iELISA and commercial ELISA test was 91.66% with Cohen's k index 0.8316 [0.710 - 0.951]. We established a cut-off value of A492nm = 0.175 for the HEV/RBD iELISA, based on the ROC curve analysis (Figure 8). The agreement between the double recognition iELISA and commercial ELISA test was 89.29% with Cohen's k index 0.7850 [0.653 - 0.917] with cut-off = 0.154.

During exposure to SARS-CoV-2, several factors may influence antibody detection. The timing of the sample is crucial since IgM usually appears first week and peaks two to three weeks after the onset of symptoms. IgG is usually found after IgM and peaks at about the same time [62]. However, the antibodies may not follow this usual pattern of seroconversion in SARS-CoV-2 infection, affected by several factors, such as the presence of memory B cells from hCoVs and cross-reactive serum antibodies [63].

However, this study has several limitations. The HEV/RBD-based iELISA, showed good specificity, but we could not assess the cross-reactivity of HEV capsid protein with anti-HEV antibodies. HEV seroprevalence ranges from 5.9% to 21.7.5% [64]. HEV capsid protein retains its ability to be recognized by HEV/RBD (Supplementary Figure 2), which would affect the specific recognition of anti-RBD antibodies in 5.9% to 21.7.5% of the population. Further, we could not assess the cross-reactivity of N protein with anti-coronaviruses that differ from SARS-CoV-2. with anti-coronaviruses that differ from SARS-CoV-2 and the influence of the plat-glycosylation model of N and HEV/RBD proteins. Nevertheless, it has been demonstrated that plant expression systems may produce functionally active SARS-CoV-2 proteins at high levels [5,31,49,58,65].

5. Conclusions

Our study confirms that the N and fusion HEV/RBD proteins transiently expressed in plants can reliably detect responses to SARS-CoV-2 in human sera. Our research validates the potential of using plants as an expression system for recombinant protein production and their application as diagnostic reagents for serological detection of infectious diseases, lowering the cost of diagnostic kits.

Supplementary Materials: The following supporting information can be downloaded at: www.mdpi.com/xxx/s1, Figure S1: title; Table S1: title; Video S1: title.

Author Contributions: Conceptualization, G.Z.; methodology, K.T.; validation, V.T., K.T., and E.S.M.; investigation, E.S.M., V.T., and K.T.; visualization, V.T.; resources, N.V.R., M.P. and S.K.; supervision, G.Z.; project administration, I.M., and G.Z.; writing—original draft preparation, G.Z.; funding acquisition, G.Z., N.V.R.; writing—review and editing, G.Z., and N.V.R. All authors have read and agreed to the published version of the manuscript."

Funding: This research was funded by the Plovdiv University research fund MUPD23-BF-002 and by the European Regional Development Fund through the Bulgarian "Science and Education for Smart Growth" Operational Program (project BG05M2OP001-1.003-0001 C04). The work of E.S.M. and N.R. was funded by the Ministry of Science and Higher Education of the Russian Federation (agreement 075-15-2022-318 dated 20 April 2022, on providing a grant for the creation and development of a World-Class Scientific Center "Agrotechnologies for the Future").

Institutional Review Board Statement: The study was conducted in accordance with the Declaration of Helsinki, and approved by the Ethics Committee of IMBB protocol code EK04-06062023.

Informed Consent Statement: Informed consent was obtained from all subjects involved in the study.

Acknowledgments: The program "Young Scientists and Postdoctoral Candidates-2" from the Bulgarian Ministry of Education and Science and L'Oréal and UNESCO initiative "For Women in Science 2022" for supporting Katerina Takova's research. Valeria Tonova thanks Prof. G.P. Lomonossoff and Dr. Keith Saunders for their support during her visit to JIC, Norwich, UK. We thank Laura Lukov, Purdue University, USA for her help with English language editing. Gergana Zahmanova thanks RIDACOM Ltd. for donation of an ELISA kit (Dia.Pro D. B., Italy).

Conflicts of Interest: The authors declare no conflicts of interest.

References

1. Ws, K.; Jh, K.; J, L.; Sy, K.; Hd, C.; I, J.; St, J.; Jh, N. Functional Expression of the Recombinant Spike Receptor Binding Domain of SARS-CoV-2 Omicron in the Periplasm of Escherichia Coli. *Bioengineering (Basel, Switzerland)* **2022**, *9*, doi:10.3390/bioengineering9110670.
2. Chen, W.-H.; Pollet, J.; Strych, U.; Lee, J.; Liu, Z.; Kundu, R.T.; Versteeg, L.; Villar, M.J.; Adhikari, R.; Wei, J.; et al. Yeast-Expressed Recombinant SARS-CoV-2 Receptor Binding Domain RBD203-N1 as a COVID-19 Protein Vaccine Candidate. *Protein Expr Purif* **2022**, *190*, 106003, doi:10.1016/j.pep.2021.106003.
3. Schaub, J.M.; Chou, C.-W.; Kuo, H.-C.; Javanmardi, K.; Hsieh, C.-L.; Goldsmith, J.; DiVenere, A.M.; Le, K.C.; Wrapp, D.; Byrne, P.O.; et al. Expression and Characterization of SARS-CoV-2 Spike Proteins. *Nat Protoc* **2021**, *16*, 5339–5356, doi:10.1038/s41596-021-00623-0.
4. Schwarze, M.; Luo, J.; Brakel, A.; Krizsan, A.; Lakowa, N.; Grünewald, T.; Lehmann, C.; Wolf, J.; Borte, S.; Milkovska-Stamenova, S.; et al. Evaluation of S- and M-Proteins Expressed in Escherichia Coli and HEK Cells for Serological Detection of Antibodies in Response to SARS-CoV-2 Infections and mRNA-Based Vaccinations. *Pathogens* **2022**, *11*, 1515, doi:10.3390/pathogens11121515.
5. Jung, J.-W.; Zahmanova, G.; Minkov, I.; Lomonossoff, G.P. Plant-Based Expression and Characterization of SARS-CoV-2 Virus-like Particles Presenting a Native Spike Protein. *Plant Biotechnology Journal* **2022**, *20*, 1363–1372, doi:10.1111/pbi.13813.
6. Ruocco, V.; Strasser, R. Transient Expression of Glycosylated SARS-CoV-2 Antigens in Nicotiana Benthamiana. *Plants* **2022**, *11*, 1093, doi:10.3390/plants11081093.
7. Zahmanova, G.; Takova, K.; Valkova, R.; Toneva, V.; Minkov, I.; Andonov, A.; Lukov, G.L. Plant-Derived Recombinant Vaccines against Zoonotic Viruses. *Life (Basel)* **2022**, *12*, 156, doi:10.3390/life12020156.
8. Ward, B.J.; Makarkov, A.; Séguin, A.; Pillet, S.; Trépanier, S.; Dhaliwall, J.; Libman, M.D.; Vesikari, T.; Landry, N. Efficacy, Immunogenicity, and Safety of a Plant-Derived, Quadrivalent, Virus-like Particle Influenza Vaccine in Adults (18–64 Years) and Older Adults (≥65 Years): Two Multicentre, Randomised Phase 3 Trials. *The Lancet* **2020**, *396*, 1491–1503, doi:10.1016/S0140-6736(20)32014-6.
9. Medicago and GSK Announce the Approval by Health Canada of COVIFENZ, an Adjuvanted Plant-Based COVID-19 Vaccine Available online: https://www.biopharminternational.com/view/medicago-and-gsk-announce-the-approval-by-health-canada-of-covifenz-an-adjuvanted-plant-based-covid-19-vaccine (accessed on 30 October 2024).
10. Mardanova, E.S.; Takova, K.H.; Toneva, V.T.; Zahmanova, G.G.; Tsybalova, L.M.; Ravin, N.V. A Plant-Based Transient Expression System for the Rapid Production of Highly Immunogenic Hepatitis E Virus-like Particles. *Biotechnol Lett* **2020**, *42*, 2441–2446, doi:10.1007/s10529-020-02995-x.
11. Zahmanova, G.; Aljabali, A.A.; Takova, K.; Toneva, V.; Tambuwala, M.M.; Andonov, A.P.; Lukov, G.L.; Minkov, I. The Plant Viruses and Molecular Farming: How Beneficial They Might Be for Human and Animal Health? *Int J Mol Sci* **2023**, *24*, 1533, doi:10.3390/ijms24021533.
12. Fischer, R.; Buyel, J.F. Molecular Farming - The Slope of Enlightenment. *Biotechnol Adv* **2020**, *40*, 107519, doi:10.1016/j.biotechadv.2020.107519.
13. Buyel, J.F.; Twyman, R.M.; Fischer, R. Extraction and Downstream Processing of Plant-Derived Recombinant Proteins. *Biotechnol Adv* **2015**, *33*, 902–913, doi:10.1016/j.biotechadv.2015.04.010.
14. Zahmanova, G.; Aljabali, A.A.A.; Takova, K.; Minkov, G.; Tambuwala, M.M.; Minkov, I.; Lomonossoff, G.P. Green Biologics: Harnessing the Power of Plants to Produce Pharmaceuticals. *Int J Mol Sci* **2023**, *24*, 17575, doi:10.3390/ijms242417575.
15. Elelyso® | Protalix Available online: https://protalix.com/products/elelyso (accessed on 30 October 2024).
16. iBio Reports Successful Preclinical Immunization Studies with Next-Gen Nucleocapsid COVID-19 Vaccine Candidate Available online: https://ir.ibioinc.com/news-events/press-releases/detail/163/ibio-reports-successful-preclinical-immunization-studies (accessed on 30 October 2024).
17. Starkevič, U.; Bortesi, L.; Virgailis, M.; Ružauskas, M.; Giritch, A.; Ražanskienė, A. High-Yield Production of a Functional Bacteriophage Lysin with Antipneumococcal Activity Using a Plant Virus-Based Expression System. *J Biotechnol* **2015**, *200*, 10–16, doi:10.1016/j.jbiotec.2015.02.028.
18. Ac, W.; Yj, P.; Ma, T.; A, W.; At, M.; D, V. Structure, Function, and Antigenicity of the SARS-CoV-2 Spike Glycoprotein. *Cell* **2020**, *181*, doi:10.1016/j.cell.2020.02.058.
19. Meyer, B.; Drosten, C.; Müller, M.A. Serological Assays for Emerging Coronaviruses: Challenges and Pitfalls. *Virus Res* **2014**, *194*, 175–183, doi:10.1016/j.virusres.2014.03.018.
20. Wang, M.-Y.; Zhao, R.; Gao, L.-J.; Gao, X.-F.; Wang, D.-P.; Cao, J.-M. SARS-CoV-2: Structure, Biology, and Structure-Based Therapeutics Development. *Front Cell Infect Microbiol* **2020**, *10*, 587269, doi:10.3389/fcimb.2020.587269.
21. Shang, J.; Wan, Y.; Luo, C.; Ye, G.; Geng, Q.; Auerbach, A.; Li, F. Cell Entry Mechanisms of SARS-CoV-2. *Proc Natl Acad Sci U S A* **2020**, *117*, 11727–11734, doi:10.1073/pnas.2003138117.
22. Cong, Y.; Ulasli, M.; Schepers, H.; Mauthe, M.; V'kovski, P.; Kriegenburg, F.; Thiel, V.; de Haan, C.A.M.; Reggiori, F. Nucleocapsid Protein Recruitment to Replication-Transcription Complexes Plays a Crucial Role in Coronaviral Life Cycle. *J Virol* **2020**, *94*, e01925-19, doi:10.1128/JVI.01925-19.

23. Chang, C.; Chen, C.-M.M.; Chiang, M.; Hsu, Y.; Huang, T. Transient Oligomerization of the SARS-CoV N Protein – Implication for Virus Ribonucleoprotein Packaging. *PLoS One* **2013**, *8*, e65045, doi:10.1371/journal.pone.0065045.
24. Kang, S.; Yang, M.; Hong, Z.; Zhang, L.; Huang, Z.; Chen, X.; He, S.; Zhou, Z.; Zhou, Z.; Chen, Q.; et al. Crystal Structure of SARS-CoV-2 Nucleocapsid Protein RNA Binding Domain Reveals Potential Unique Drug Targeting Sites. *Acta Pharm Sin B* **2020**, *10*, 1228–1238, doi:10.1016/j.apsb.2020.04.009.
25. Tilocca, B.; Soggiu, A.; Sanguinetti, M.; Musella, V.; Britti, D.; Bonizzi, L.; Urbani, A.; Roncada, P. Comparative Computational Analysis of SARS-CoV-2 Nucleocapsid Protein Epitopes in Taxonomically Related Coronaviruses. *Microbes Infect* **2020**, *22*, 188–194, doi:10.1016/j.micinf.2020.04.002.
26. Zhou, P.; Yang, X.-L.; Wang, X.-G.; Hu, B.; Zhang, L.; Zhang, W.; Si, H.-R.; Zhu, Y.; Li, B.; Huang, C.-L.; et al. A Pneumonia Outbreak Associated with a New Coronavirus of Probable Bat Origin. *Nature* **2020**, *579*, 270–273, doi:10.1038/s41586-020-2012-7.
27. Wu, W.; Cheng, Y.; Zhou, H.; Sun, C.; Zhang, S. The SARS-CoV-2 Nucleocapsid Protein: Its Role in the Viral Life Cycle, Structure and Functions, and Use as a Potential Target in the Development of Vaccines and Diagnostics. *Virol J* **2023**, *20*, 6, doi:10.1186/s12985-023-01968-6.
28. Rockstroh, A.; Wolf, J.; Fertey, J.; Kalbitz, S.; Schroth, S.; Lübbert, C.; Ulbert, S.; Borte, S. Correlation of Humoral Immune Responses to Different SARS-CoV-2 Antigens with Virus Neutralizing Antibodies and Symptomatic Severity in a German COVID-19 Cohort. *Emerg Microbes Infect* **2021**, *10*, 774–781, doi:10.1080/22221751.2021.1913973.
29. Atyeo, C.; Fischinger, S.; Zohar, T.; Slein, M.D.; Burke, J.; Loos, C.; McCulloch, D.J.; Newman, K.L.; Wolf, C.; Yu, J.; et al. Distinct Early Serological Signatures Track with SARS-CoV-2 Survival. *Immunity* **2020**, *53*, 524-532.e4, doi:10.1016/j.immuni.2020.07.020.
30. Infantino, M.; Damiani, A.; Gobbi, F.L.; Grossi, V.; Lari, B.; Macchia, D.; Casprini, P.; Veneziani, F.; Villalta, D.; Bizzaro, N.; et al. Serological Assays for SARS-CoV-2 Infectious Disease: Benefits, Limitations and Perspectives. *Isr Med Assoc J* **2020**, *22*, 203–210.
31. Mamedov, T.; Yuksel, D.; Gurbuzaslan, I.; Ilgin, M.; Gulec, B.; Mammadova, G.; Ozdarendeli, A.; Pavel, S.T.I.; Yetiskin, H.; Kaplan, B.; et al. Plant-Produced RBD and Cocktail-Based Vaccine Candidates Are Highly Effective against SARS-CoV-2, Independently of Its Emerging Variants. *Front Plant Sci* **2023**, *14*, 1202570, doi:10.3389/fpls.2023.1202570.
32. Mamedov, T.; Yuksel, D.; Ilgın, M.; Gürbüzaslan, I.; Gulec, B.; Mammadova, G.; Ozdarendeli, A.; Yetiskin, H.; Kaplan, B.; Islam Pavel, S.T.; et al. Production and Characterization of Nucleocapsid and RBD Cocktail Antigens of SARS-CoV-2 in Nicotiana Benthamiana Plant as a Vaccine Candidate against COVID-19. *Vaccines (Basel)* **2021**, *9*, 1337, doi:10.3390/vaccines9111337.
33. Santoni, M.; Gutierrez-Valdes, N.; Pivotto, D.; Zanichelli, E.; Rosa, A.; Sobrino-Mengual, G.; Balieu, J.; Lerouge, P.; Bardor, M.; Cecchetto, R.; et al. Performance of Plant-Produced RBDs as SARS-CoV-2 Diagnostic Reagents: A Tale of Two Plant Platforms. *Front Plant Sci* **2023**, *14*, 1325162, doi:10.3389/fpls.2023.1325162.
34. Mardanova, E.S.; Kotlyarov, R.Y.; Stuchinskaya, M.D.; Nikolaeva, L.I.; Zahmanova, G.; Ravin, N.V. High-Yield Production of Chimeric Hepatitis E Virus-Like Particles Bearing the M2e Influenza Epitope and Receptor Binding Domain of SARS-CoV-2 in Plants Using Viral Vectors. *Int J Mol Sci* **2022**, *23*, 15684, doi:10.3390/ijms232415684.
35. Zahmanova, G.G.; Mazalovska, M.; Takova, K.H.; Toneva, V.T.; Minkov, I.N.; Mardanova, E.S.; Ravin, N.V.; Lomonossoff, G.P. Rapid High-Yield Transient Expression of Swine Hepatitis E ORF2 Capsid Proteins in Nicotiana Benthamiana Plants and Production of Chimeric Hepatitis E Virus-Like Particles Bearing the M2e Influenza Epitope. *Plants (Basel)* **2019**, *9*, 29, doi:10.3390/plants9010029.
36. Mardanova, E.S.; Vasyagin, E.A.; Kotova, K.G.; Zahmanova, G.G.; Ravin, N.V. Plant-Produced Chimeric Hepatitis E Virus-like Particles as Carriers for Antigen Presentation. *Viruses* **2024**, *16*, 1093, doi:10.3390/v16071093.
37. Hussain, H.; Maldonado-Agurto, R.; Dickson, A.J. The Endoplasmic Reticulum and Unfolded Protein Response in the Control of Mammalian Recombinant Protein Production. *Biotechnol Lett* **2014**, *36*, 1581–1593, doi:10.1007/s10529-014-1537-y.
38. Whitman, J.D.; Hiatt, J.; Mowery, C.T.; Shy, B.R.; Yu, R.; Yamamoto, T.N.; Rathore, U.; Goldgof, G.M.; Whitty, C.; Woo, J.M.; et al. Evaluation of SARS-CoV-2 Serology Assays Reveals a Range of Test Performance. *Nat Biotechnol* **2020**, *38*, 1174–1183, doi:10.1038/s41587-020-0659-0.
39. Tré-Hardy, M.; Wilmet, A.; Beukinga, I.; Favresse, J.; Dogné, J.-M.; Douxfils, J.; Blairon, L. Analytical and Clinical Validation of an ELISA for Specific SARS-CoV-2 IgG, IgA, and IgM Antibodies. *J Med Virol* **2021**, *93*, 803–811, doi:10.1002/jmv.26303.
40. Sainsbury, F.; Thuenemann, E.C.; Lomonossoff, G.P. pEAQ: Versatile Expression Vectors for Easy and Quick Transient Expression of Heterologous Proteins in Plants. *Plant Biotechnol J* **2009**, *7*, 682–693, doi:10.1111/j.1467-7652.2009.00434.x.

41. Zhao, H.; Nguyen, A.; Wu, D.; Li, Y.; Hassan, S.A.; Chen, J.; Shroff, H.; Piszczek, G.; Schuck, P. Plasticity in Structure and Assembly of SARS-CoV-2 Nucleocapsid Protein. *bioRxiv* **2022**, 2022.02.08.479556, doi:10.1101/2022.02.08.479556.
42. Abebe, E.C.; Dejenie, T.A. Protective Roles and Protective Mechanisms of Neutralizing Antibodies against SARS-CoV-2 Infection and Their Potential Clinical Implications. *Front Immunol* **2023**, *14*, 1055457, doi:10.3389/fimmu.2023.1055457.
43. Gao, T.; Gao, Y.; Liu, X.; Nie, Z.; Sun, H.; Lin, K.; Peng, H.; Wang, S. Identification and Functional Analysis of the SARS-COV-2 Nucleocapsid Protein. *BMC Microbiol* **2021**, *21*, 58, doi:10.1186/s12866-021-02107-3.
44. Ju, B.; Zhang, Q.; Ge, J.; Wang, R.; Sun, J.; Ge, X.; Yu, J.; Shan, S.; Zhou, B.; Song, S.; et al. Human Neutralizing Antibodies Elicited by SARS-CoV-2 Infection. *Nature* **2020**, *584*, 115–119, doi:10.1038/s41586-020-2380-z.
45. Kolesov, D.E.; Sinegubova, M.V.; Dayanova, L.K.; Dolzhikova, I.V.; Vorobiev, I.I.; Orlova, N.A. Fast and Accurate Surrogate Virus Neutralization Test Based on Antibody-Mediated Blocking of the Interaction of ACE2 and SARS-CoV-2 Spike Protein RBD. *Diagnostics (Basel)* **2022**, *12*, 393, doi:10.3390/diagnostics12020393.
46. Fox, T.; Geppert, J.; Dinnes, J.; Scandrett, K.; Bigio, J.; Sulis, G.; Hettiarachchi, D.; Mathangasinghe, Y.; Weeratunga, P.; Wickramasinghe, D.; et al. Antibody Tests for Identification of Current and Past Infection with SARS-CoV-2. *Cochrane Database Syst Rev* **2022**, *11*, CD013652, doi:10.1002/14651858.CD013652.pub2.
47. Spencer, K.-A.; Osorio, F.A.; Hiscox, J.A. Recombinant Viral Proteins for Use in Diagnostic ELISAs to Detect Virus Infection. *Vaccine* **2007**, *25*, 5653, doi:10.1016/j.vaccine.2007.02.053.
48. Yin, J.; Li, G.; Ren, X.; Herrler, G. Select What You Need: A Comparative Evaluation of the Advantages and Limitations of Frequently Used Expression Systems for Foreign Genes. *J Biotechnol* **2007**, *127*, 335–347, doi:10.1016/j.jbiotec.2006.07.012.
49. Williams, L.; Jurado, S.; Llorente, F.; Romualdo, A.; González, S.; Saconne, A.; Bronchalo, I.; Martínez-Cortes, M.; Pérez-Gómez, B.; Ponz, F.; et al. The C-Terminal Half of SARS-CoV-2 Nucleocapsid Protein, Industrially Produced in Plants, Is Valid as Antigen in COVID-19 Serological Tests. *Frontiers in Plant Science* **2021**, *12*, 699665, doi:10.3389/fpls.2021.699665.
50. Mazalovska, M.; Varadinov, N.; Koynarski, T.; Minkov, I.; Teoharov, P.; Lomonossoff, G.P.; Zahmanova, G. Detection of Serum Antibodies to Hepatitis E Virus Based on HEV Genotype 3 ORF2 Capsid Protein Expressed in Nicotiana Benthamiana. *Annals of Laboratory Medicine* **2017**, *37*, 313, doi:10.3343/alm.2017.37.4.313.
51. Takova, K.; Koynarski, T.; Minkov, G.; Toneva, V.; Mardanova, E.; Ravin, N.; Lukov, G.L.; Zahmanova, G. Development and Optimization of an Enzyme Immunoassay to Detect Serum Antibodies against the Hepatitis E Virus in Pigs, Using Plant-Derived ORF2 Recombinant Protein. *Vaccines* **2021**, *9*, 991, doi:10.3390/vaccines9090991.
52. Goulet, M.-C.; Gaudreau, L.; Gagné, M.; Maltais, A.-M.; Laliberté, A.-C.; Éthier, G.; Bechtold, N.; Martel, M.; D'Aoust, M.-A.; Gosselin, A.; et al. Production of Biopharmaceuticals in Nicotiana Benthamiana—Axillary Stem Growth as a Key Determinant of Total Protein Yield. *Frontiers in Plant Science* **2019**, *10*, 735, doi:10.3389/fpls.2019.00735.
53. Peyret, H.; Steele, J.F.C.; Jung, J.-W.; Thuenemann, E.C.; Meshcheriakova, Y.; Lomonossoff, G.P. Producing Vaccines against Enveloped Viruses in Plants: Making the Impossible, Difficult. *Vaccines (Basel)* **2021**, *9*, 780, doi:10.3390/vaccines9070780.
54. Castilho, A.; Schwestka, J.; Kienzl, N.F.; Vavra, U.; Grünwald-Gruber, C.; Izadi, S.; Hiremath, C.; Niederhöfer, J.; Laurent, E.; Monteil, V.; et al. Generation of Enzymatically Competent SARS-CoV-2 Decoy Receptor ACE2-Fc in Glycoengineered Nicotiana Benthamiana. *Biotechnology Journal* **2021**, *16*, 2000566, doi:10.1002/biot.202000566.
55. Puchol Tarazona, A.A.; Maresch, D.; Grill, A.; Bakalarz, J.; Torres Acosta, J.A.; Castilho, A.; Steinkellner, H.; Mach, L. Identification of Two Subtilisin-like Serine Proteases Engaged in the Degradation of Recombinant Proteins in Nicotiana Benthamiana. *FEBS Lett* **2021**, *595*, 379–388, doi:10.1002/1873-3468.14014.
56. Shajahan, A.; Pepi, L.E.; Rouhani, D.S.; Heiss, C.; Azadi, P. Glycosylation of SARS-CoV-2: Structural and Functional Insights. *Anal Bioanal Chem* **2021**, 7179–7193.
57. Watanabe, Y.; Berndsen, Z.T.; Raghwani, J.; Seabright, G.E.; Allen, J.D.; Pybus, O.G.; McLellan, J.S.; Wilson, I.A.; Bowden, T.A.; Ward, A.B.; et al. Vulnerabilities in Coronavirus Glycan Shields despite Extensive Glycosylation. *Nat Commun* **2020**, *11*, 2688, doi:10.1038/s41467-020-16567-0.
58. Capell, T.; Twyman, R.M.; Armario-Najera, V.; Ma, J.K.-C.; Schillberg, S.; Christou, P. Potential Applications of Plant Biotechnology against SARS-CoV-2. *Trends Plant Sci* **2020**, *25*, 635–643, doi:10.1016/j.tplants.2020.04.009.
59. Márquez-Ipiña, A.R.; González-González, E.; Rodríguez-Sánchez, I.P.; Lara-Mayorga, I.M.; Mejía-Manzano, L.A.; Sánchez-Salazar, M.G.; González-Valdez, J.G.; Ortiz-López, R.; Rojas-Martínez, A.; Trujillo-de Santiago, G.; et al. Serological Test to Determine Exposure to SARS-CoV-2: ELISA Based on the Receptor-

Binding Domain of the Spike Protein (S-RBDN318-V510) Expressed in Escherichia Coli. *Diagnostics* **2021**, *11*, 271, doi:10.3390/diagnostics11020271.

60. Khan, W.H.; Khan, N.; Mishra, A.; Gupta, S.; Bansode, V.; Mehta, D.; Bhambure, R.; Ansari, M.A.; Das, S.; Rathore, A.S. Dimerization of SARS-CoV-2 Nucleocapsid Protein Affects Sensitivity of ELISA Based Diagnostics of COVID-19. *International Journal of Biological Macromolecules* **2022**, *200*, 428, doi:10.1016/j.ijbiomac.2022.01.094.
61. Avdjieva, I.; Terziyski, I.; Zahmanova, G.; Simeonova, V.; Kulev, O.; Krastev, E.; Krachunov, M.; Nisheva-Pavlova, M.; Vassilev, D. HOMOLOGY BASED COMPUTATIONAL MODELLING OF HEPATITIS-E VIRAL FUSION CAPSID PROTEIN. **2019**, doi:10.7546/CRABS.2019.03.10.
62. Long, Q.-X.; Liu, B.-Z.; Deng, H.-J.; Wu, G.-C.; Deng, K.; Chen, Y.-K.; Liao, P.; Qiu, J.-F.; Lin, Y.; Cai, X.-F.; et al. Antibody Responses to SARS-CoV-2 in Patients with COVID-19. *Nat Med* **2020**, *26*, 845–848, doi:10.1038/s41591-020-0897-1.
63. Morgenlander, W.R.; Henson, S.N.; Monaco, D.R.; Chen, A.; Littlefield, K.; Bloch, E.M.; Fujimura, E.; Ruczinski, I.; Crowley, A.R.; Natarajan, H.; et al. Antibody Responses to Endemic Coronaviruses Modulate COVID-19 Convalescent Plasma Functionality. *J Clin Invest* **2021**, *131*, e146927, 146927, doi:10.1172/JCI146927.
64. Zahmanova, G.; Takova, K.; Tonova, V.; Koynarski, T.; Lukov, L.L.; Minkov, I.; Pishmisheva, M.; Kotsev, S.; Tsachev, I.; Baymakova, M.; et al. The Re-Emergence of Hepatitis E Virus in Europe and Vaccine Development. *Viruses* **2023**, *15*, 1558, doi:10.3390/v15071558.
65. Maharjan, P.M.; Cheon, J.; Jung, J.; Kim, H.; Lee, J.; Song, M.; Jeong, G.U.; Kwon, Y.; Shim, B.; Choe, S. Plant-Expressed Receptor Binding Domain of the SARS-CoV-2 Spike Protein Elicits Humoral Immunity in Mice. *Vaccines (Basel)* **2021**, *9*, 978, doi:10.3390/vaccines9090978.